Published in final edited form as:

Cancer Res. 2012 March 15; 72(6): 1384–1394. doi:10.1158/0008-5472.CAN-11-2905.

Myeloid progenitor cells in the premetastatic lung promote metastases by inducing mesenchymal to epithelial transition.

Dingcheng Gao[1,2], **Natasha Joshi**[1,2], **Hyejin Choi**[1,2], **Seongho Ryu**[1,2], **Mary Hahn**[1,2], **Raul Catena**[1,2], **Helen Sadik**[6], **Pedram Argani**[6], **Patrick Wagner**[3], **Linda T. Vahdat**[4], **Jeffrey L. Port**[1], **Brendon Stiles**[1], **Saraswati Sukumar**[6], **Nasser K. Altorki**[1], **Shahin Rafii**[5], **Vivek Mittal**[1,2]

[1]Department of Cardiothoracic Surgery and Neuberger Berman Lung Cancer Center, Weill Cornell Medical College of Cornell University, 1300 York Avenue, 525 East 68th street, New York, New York 10065

[2]Department of Cell and Developmental Biology, Weill Cornell Medical College of Cornell University, 1300 York Avenue, 525 East 68th street, New York, New York 10065

[3]Department of Pathology, Weill Cornell Medical College of Cornell University, 1300 York Avenue, 525 East 68th street, New York, New York 10065

[4]Department of Medicine, Weill Cornell Medical College of Cornell University, 1300 York Avenue, 525 East 68th street, New York, New York 10065

[5]HHMI, Department of Genetic Medicine, Weill Cornell Medical College of Cornell University, 1300 York Avenue, 525 East 68th street, New York, New York 10065

[6]Sidney Kimmel Comprehensive Cancer Center at Johns Hopkins, 1650 Orleans Street, Baltimore, MD 21231-1000

Abstract

Tumors systemically initiate metastatic niches in distant target metastatic organs. These niches, comprised of bone marrow (BM)-derived hematopoietic cells, provide permissive conditions for future metastases. However, the mechanisms by which these cells mediate outgrowth of metastatic tumor cells are not completely known. Using mouse models of spontaneous breast cancer, we show enhanced recruitment of BM-derived $CD11b^{+}Gr1^{+}$ myeloid progenitor cells in the premetastatic lungs. Gene expression profiling revealed that the myeloid cells from metastatic lungs express versican, an extracellular matrix proteoglycan. Notably, versican in metastatic lungs was mainly contributed by the $CD11b^{+}Ly6C^{high}$ monocytic fraction of the myeloid cells and not the tumor cells or other stromal cells. Versican knockdown in the BM significantly impaired lung metastases in vivo, without impacting their recruitment to the lungs or altering the immune microenvironment. Versican stimulated mesenchymal to epithelial transition (MET) of metastatic tumor cells by attenuating phospho-Smad2 levels, which resulted in elevated cell proliferation and accelerated metastases. Analysis of clinical specimens showed elevated versican expression within the metastatic lung of breast cancer patients. Together, our findings suggest that selectively

Correspondence: Vivek Mittal, Weill Cornell Medical College of Cornell University, 1300 York Avenue, Room 603C, New York, NY 10065; Dingcheng Gao, Weill Cornell Medical College of Cornell University, 1300 York Avenue, Room 603A, New York, NY 10065.

targeting tumor elicited myeloid cells or versican represents a potential therapeutic strategy for combating metastatic disease.

Keywords

Bone marrow; Myeloid cells; Metastasis; Ly6C; Versican; Mesenchymal to epithelial transition

Introduction

Malignant tumors colonize distal target organs to establish metastases (1, 2) causing more than 90% of human cancer-related deaths (3). Many studies have investigated the cancer cell intrinsic molecular mechanisms and the extrinsic microenvironmental factors that enhance the metastatic potential of primary tumor cells (3, 4). Notably, activation of EMT, a developmental program, endows metastatic properties upon cancer cells to promote invasion, migration, and subsequent dissemination (5).

Following dissemination, the establishment of metastatic lesions depends on the organ-colonizing properties of disseminated tumor cells as well as on permissive conditions or the “metastatic niche” that may be present in the microenvironment of target organs (3, 6). Notably, BM-derived cells are recruited to the metastatic organs to support initiation of metastases (7), and angiogenesis-mediated progression of micrometastases to macrometastases (8). Although some of these stromal contributors have been identified, effective therapies still require a more comprehensive understanding of the complex molecular and cellular network of tumor-stromal interactions in the metastatic organ that contribute to the formation of macrometastases. Transitions between epithelial and mesenchymal states have crucial roles both in embryonic development and cancer. An apparent contradiction of the association between EMT and metastasis comes from repeated observations that distant metastases derived from primary carcinomas are largely composed of cancer cells showing an epithelial phenotype closely resembling that of the cancer cells in the primary tumor. This has led to speculation that the disseminated mesenchymal tumor cells recruited to the target organs may undergo mesenchymal to epithelial transition (MET) which would favor metastases formation (9). However, the MET cascade has not been recapitulated in animal models, and the cellular and molecular regulators that promote MET remain unknown. In this study, we have focused on events in the distal metastatic organ and sought to identify the microenvironmental factors that affect metastatic outgrowth.

Materials and Methods

Mice:

FVB/n, FVB.Cg-Tg (ACTB-EGFP) B5Nagy/J, and MMTV-PyVT mice were obtained from The Jackson Laboratory (Bar Harbor, Maine). Male MMTV-PyMT transgenic mice were bred with wild type FVB/N females. Female off-springs (3 weeks) were genotyped to identify mice carrying the PyMT transgene. The positive mice spontaneously develop mammary tumors by 6-7 weeks of age and pulmonary metastases by 10-12 weeks of age. To quantify lung metastases in MMTV-PyMT mice, serial lung sections (at least 10) were

prepared and stained with Hematoxylin & Eosin (HE). Within the stained sections, areas depicting metastatic lesions and total lung were measured with ImageJ software.

Cell lines:

The human breast cancer cell line (MDA-MB-231) was obtained from ATCC, a kind gift from Dr. Randy Watnick (Harvard Medical School, Boston, MA). Cultures were resuscitated from stocks frozen at low passage within 6-month of purchase. Cell authentication was performed at ATCC by short tandem repeat (STR) profiling, cell morphology monitoring, karyotyping and the ATCC COI assays. The morphology and metastatic behavior of MDA-MB-231 cells were tested in our lab and Dr. Watnick's lab. Cells were cultured in DMEM with 10% fetal bovine serum, 5 mmol/L glutamine, and 1% penicillin/streptomycin. Versican-expressing cells (MDA-Vcn) were generated by transfection with a construct carrying the secreted form of human versican cDNA (pSecTag-V1, a gift from Dr. Zimmermann, University of Zurich) (10). Stably transfected cells were obtained by selecting cells with Zeocin (200 ng/mL). MDA-Cont cells were obtained by transfection of MDA-MB-231 cells with control empty vector and selected through the same procedure. MDA-MB-231 cells were also labeled with luciferase-RFP fusion protein for bioluminescent imaging *in vivo*.

Human samples:

Human normal lung tissues (n=5) were obtained from ILSbio LLC (Chestertown, MD). Human lungs bearing metastases from breast cancer patients were obtained from CT Surgery Department, Weill Cornell Medical College, consented according to approved IRB protocols from the institution. Metastatic tissues from the lungs of breast cancer patients (n=11) were obtained in the form of a tissue microarray from Dr. Pedram Argani and Dr. Sara Sukumar's group at Johns Hopkins University School of Medicine, Baltimore.

Short hairpin RNA design, and lentiviral vector generation:

Mir30 based shRNAs targeting mouse versican (V0/V1 isoform) were designed, and cloned into the Xho I/EcoR I site of the lentiviral construct pGIPZ (OpenBiosystem). Multiple hairpin constructs were screened for effective knockdown of versican. The 22mer targeting sequence that resulted in efficient knockdown included 5'-ACACCAGAATTAGAAAGTTCAA-3' (shVcn1) and 5'-AGCACCTTGTCTGATGGCCAAG-3' (shVcn2), shRNA targeting firefly luciferase served as a non-specific control. Lentivirus was generated and concentrated using standard protocols. Lentiviral transductions of Lin^- BM cells were performed as described (8).

BM transplantation of mice:

BM cells were harvested by flushing femurs and tibias of donor animals. BM transplantation was performed by injecting 1×10^7 total BM cells via tail vein into lethally irradiated (900 rads) recipients as described (8).

Immunostaining and microscopy:

Fixed tissue sections (30 μm) were stained with fluorescence labeled antibodies against CD11b (clone ICRF44.), CD33 (Cat#555459, BD), Gr1 (Clone RB6-8C5), Versican (Cat#V5639, Sigma and Clone 2B1 Seikagaku), PyMT (NB 100-2749, Novus) according to standard protocols. Fluorescent images were obtained using an Axiovert 200M fluorescent microscope (Carl Zeiss Inc.). For versican staining, sections were first treated with chondroitinase ABC (Sigma) overnight and then incubated with an anti-versican antibody (Cat#V5639, Sigma). For IHC, the antibody labeling was visualized using the DAKO Envision™ system (DAKO). Images were taken with an Olympus BX51 microscope coupled with Qcapture software (Olympus).

Conditioned medium, purified versican and cell proliferation assay:

Flow cytometry sorted $CD11b^{+}Gr1^{+}$ cells from MMTV-PyMT mice (10-weeks old) were cultured in RPMI with 10% FBS with a density of 100,000 cells/mL in 6-well plates. Conditioned medium was harvested after 2 days. For versican purification, 293T cells were transfected with construct carrying 6×His tagged human versican (V1 isoform). Supernatant was harvested 5 days after transfection. Versican was purified with Ni-NTA Fast Start Kit (Qiagen Inc). For cell proliferation assay, cells were treated with the conditioned medium, purified versican (2.5 μg/mL), or normal growth medium for 3 days. EdU (10nM) was administrated to culture medium for 30 min. The incorporation of EdU was detected using the Click-iT® EdU Cell Proliferation Assay kit (Invitrogen Inc) and analyzed by flow cytometry.

Statistical Analysis:

Results are expressed as mean ± standard deviation (s.d.). Analyses of different treatment groups were performed using the Mann-Whitney T test using the GraphPad Prism statistical program. P values < 0.05 were considered significant. Error bars depict s.d., except indicated otherwise.

Supplementary methods

Supplementary methods include flow cytometry analysis, quantitative RT-PCR analysis including primer sequences (Table S1) and western blot analysis.

Results

BM-derived $CD11b^{+}Gr1^{+}$ myeloid cells are recruited in the metastatic lungs.

To determine the contribution of the BM-derived cells to the metastatic lung, we transplanted MMTV-PyMT transgenic mice (11) with syngeneic GFP^{+} BM as previously described (8, 12). In these animals, spontaneous breast tumors (6-7 weeks of age) metastasize to the lungs and form micrometastases (11-12 weeks of age), and macrometastases by week16 (8, 12). Flow cytometry analysis showed increased recruitment (~3fold) of GFP^{+} BM-derived cells in the MMTV-PyMT metastatic lungs compared to wild type (WT) (36.3 ± 4.3% and 12.4 ± 4.2% of total lung cells respectively, Figure 1A). Notably, in the metastatic lung, the recruited GFP^{+} BM-derived cells were predominantly

$CD11b^+Gr1^+$ myeloid progenitor cells (>50%, Figure 1A) as determined by flow cytometry and immunostaining (Figure 1B).

We next performed a kinetic analysis to determine the recruitment of these cells as a function of metastases progression. Notably, the recruitment of $CD11b^+Gr1^+$ cells was observed in the premetastatic lung of 8-week old MMTV-PyMT mice before the appearance of metastases, and increasing numbers of $CD11b^+Gr1^+$ cells were associated with the progression of metastases (Figure 1C and Figure S1). Conspicuously, compared to the metastatic lung, the numbers of $CD11b^+Gr1^+$ myeloid cells were less abundant in the primary tumor. The $CD11b^+$ cells in primary tumor tissue were predominantly $Gr1^-F4/80^+$ macrophages (approximately 80%) in contrast to the $Gr1^+F4/80^-$ myeloid cells in metastatic lung (Fig. 1D). Such enhanced recruitment of myeloid cells specifically in the metastatic lungs suggests that they may be involved in promoting outgrowth of tumor cells.

Versican is expressed by myeloid cells in the metastatic lung.

To determine the molecular mechanisms by which the $CD11b^+Gr1^+$ myeloid cells may contribute to lung metastasis, we performed gene expression profiling of flow cytometry sorted $CD11b^+Gr1^+$ cells from metastatic and WT lungs. A cluster of differentially upregulated genes was identified in the myeloid cells from metastatic lungs (Figure 2A). Of the candidate genes, we focused on versican, an extracellular matrix (ECM) chondroitin sulfate proteoglycan (13), expressed by tumor stromal cells (14-19). However, the biological function of versican *in vivo* particularly in the metastatic organs has not been elucidated. RT-PCR analysis showed an approximately 5-fold increase in versican expression in the metastatic lung (ML, total) compared to controls (WT, total) (Figure 2B). In the metastatic lungs versican expression was confined to $CD11b^+Gr1^+$ cells and not to the $CD11b^-Gr1^-$ stromal cells including subsets of T and B cells (Figure 2B). Consistent with RT-PCR, western blot analysis showed elevated versican protein in the metastatic lung compared to WT controls (Figure 2C).

Flow analysis showed that the $CD11b^+Gr1^+$ cells are comprised of $CD11b^+Ly6C^{high}$ and $CD11b^+Ly6G^{high}$ subpopulations (Figure 2D) (20-22), and their recruitment increased as a function of metastatic progression (Figure S2A, S2B). Interestingly, versican expression was confined to the $Ly6C^{high}$ cells (Figure 2E). Nuclear morphology analysis showed that the $CD11b^+Ly6C^{high}$ cells are mononuclear, while the $CD11b^+Ly6G^{high}$ cells are polymorphonuclear (Figure 2F). Consistently, versican protein was also detected in the mononuclear $CD11b^+Ly6C^{high}$ cells by immunohistochemical and Western blot analyses (Figure 2F,G). In the primary tumors, versican was also confined to the low abundance $CD11b^+Ly6C^{high}$ myeloid cells, while the abundant $CD11b^+F4/80^+$ myeloid cells did not express versican (Figure S3).

Contrary to previous studies using cultured cell lines (23-25), endothelial cells and the fibroblasts did not show significant versican levels compared to $CD11b^+Ly6C^{high}$ cells in the metastatic lungs (Figure S4A). Importantly, the contribution of fibroblasts to the metastatic lung was about 10-fold lower compared to $CD11b^+Ly6C^{high}$ cells, and no significant increase in numbers was observed in the metastatic lungs compared to controls (Figure S4B). Furthermore, analysis a panel of tumor cell lines showed significantly lower versican

expression compared with sorted myeloid cells (Figure S4C). Taken together, these results suggest that the Ly6C^{high} myeloid cells are the major contributors of versican in metastatic lungs.

Versican suppression in myeloid cells impairs lung metastases.

To explore the role of myeloid cell-derived versican in pulmonary metastasis, we performed versican knockdown in BM cells *in vivo*. Given that versican is confined to the CD11b^{+}Ly6C^{high} myeloid cells, we reasoned that versican knockdown in total BM cells would only impact the Ly6C^{high} cells, thereby providing exquisite specificity. Two short hairpin RNAs (shRNA) specifically targeting exon 8 (V0/V1 specific exon) were generated (Figure S5A-B), which effectively reduced endogenous versican (V0/V1) expression as compared to non-specific shRNA control (Figure S5C).

Versican-specific shRNA (shVcn) or non-specific shRNA (shNS) was introduced via. lentiviruses into lineage WT negative (Lin^{-}) BM progenitor cells and then transplanted into lethally irradiated MMTV-PyMT recipient mice (4-weeks old) as described in our previous studies (8, 12). Successful BM reconstitution was confirmed by flow analysis of transplanted recipient mice (Figure S6A). In the lungs, as expected, versican expression was upregulated (>3 fold) in shNS-BMT MMTV-PyMT mice compared to controls (Figure S6B). However, versican expression was inhibited in shVcn-BMT mice (Figure S6B). Versican knockdown in the recruited Gr1^{+} cells in the lungs of shVcn-BMT mice (Figure 3A, 3B), resulted in impaired lung metastases compared with shNS-BMT controls (0.60 ± 0.25% vs. 12.8 ± 3.2%, respectively, Figure 3C,D). Immunohistochemical examination of the lungs from shVcn-BMT animals showed severe impairment of macrometastases while micrometastases remained unaffected (Figure 3E, Figure S7), while the primary breast tumors remained unaffected in these mice. Taken together, these results demonstrate that versican deficiency in the recruited myeloid cells significantly impaired tumor outgrowth at the metastatic site.

Myeloid cell-derived versican enhances proliferation of metastatic tumor cells to promote outgrowth

Versican knockdown did not affect the recruitment of CD11b^{+}Gr1^{+} myeloid cells in the lung microenvironment as determined by immunostaining (Figure 3A) and flow cytometry (15.8± 1.9% in shRNA-BMT vs. 15.3 ± 4.2% in shVcn-BMT mice, Figure S8A, 8B), nor did it perturb the recruitment of other BM cells including B cells (B220^{+}) or T cells (CD3^{+}) (Figure S8A,S8B). As expected, the immune microenvironment of the lungs remained unperturbed as a result of versican knockdown as evaluated by expression of key mediators including TNF-α, IL-1, IL-6, IL-4, IL-10, Arginase 1, Arginase 2, and NOS2 (Figure S8C), suggesting that versican deficiency did not affect MDSC activity of myeloid cells. Taken together, these results suggest a novel function for these myeloid progenitor cells in promoting metastases.

Previous studies have shown that versican V1 promotes cell proliferation in NIH3T3 fibroblasts (25). Therefore, we posited that versican expressed by recruited myeloid cells might enhance proliferation of metastatic tumor cells to promote tumor outgrowth. Consistent with this hypothesis, abundant Ki67^{+} proliferating cells were observed in

metastatic lesions in shNS-BMT mice where versican was available, compared with metastatic lesions from shVcn-BMT mice where versican expression was suppressed (Figure 3F-G, Figure S9A).

Taken together, these results demonstrate that versican deficiency in the BM does not affect the recruitment of $CD11b^{+}Gr1^{+}$ cells and other immune cells to the lung microenvironment. However, versican expressed by these myeloid cells promotes metastatic tumor outgrowth by enhancing cell proliferation.

Versican promotes proliferation and induces mesenchymal to epithelial transition of metastatic tumor cells.

To further evaluate the cell proliferation promoting function of versican, we used metastatic human breast cancer cells, MDA-MB-231. To mirror the paracrine effects of versican secreted by myeloid cells on metastatic tumor cells *in vitro*, we generated conditioned media (CM) from flow sorted $CD11b^{+}Gr1^{+}$ cells from the lungs of tumor-bearing mice. Administration of the Gr1 CM to MDA-MB-231 cells increased cells in S phase compared to controls (Figure 4A). Consistently, the proliferation rate of MDA-MB-231 cells was enhanced following expression of a secreted form (10) of versican V1 isoform (12.1% and 5.4% of S phase cells with and without versican respectively, Figure S9B).

Interestingly, versican-induced proliferation increase in MDA-MB-231 cells treated with Gr1 CM was associated with the acquisition of an epithelial phenotype as indicated by upregulation of epithelial cell markers including E-cadherin and occludin, and a concomitant inhibition of the mesenchymal marker vimentin (Figure 4B). These results suggested that a mesenchymal to epithelial transition (MET) had occurred in these cells, presumably mediated by versican present in the Gr1 CM. To confirm this we treated MDA-MB-231 cells with biochemically purified versican (V1 isoform) (Figure S10A, S10B), and observed induction of MET (Figure 4B). In agreement with this observation, MDA-MB-231 cell expressing a secreted form of versican (V1 isoform) established aggregated cobblestone-like colonies (Figure 4C, phase contrast top and bottom panel), and showed induction of epithelial, and suppression of mesenchymal markers as determined by immunostaining, Western blot and RT-PCR analysis (Figure 4C, 4D; Figure S11). Importantly, versican attenuated phospho (p)-Smad2 levels in MDA-MB-231 cells, while the levels of total Smad2/3 remained unchanged (Figure 4D). Given that p-Smad2 is a regulator of key EMT-promoting transcription factors including snail, it is plausible that versican-mediated attenuation of p-Smad2 levels (Figure 4D) and suppression of snail (Figure S11) in MDA-MB-231 cells may have inhibited the TGF-β-Smad2/3 signaling pathway, a well-known stimulator of EMT in various tumors (26-29). These results suggest that versican-mediated blockade of the TGFβ-Smad2 pathway may stimulate MET, resulting in increased cell proliferation which collectively promotes focal tumor outgrowth at the metastatic site.

Versican deficiency inhibits metastases *in vivo* by blocking MET.

In tumor progression, EMT confers an invasive and metastatic phenotype that supports escape of tumor cells from the primary tumor site. It is speculated that subsequently, the disseminated mesenchymal tumor cells must undergo the reverse transition, MET,

at the site of metastasis, as metastases recapitulate the pathology of their corresponding primary tumors (9, 30, 31). However, MET has not been accurately recapitulated in breast cancer metastasis. To assess if MET occurs *in vivo*, we inoculated MDA-MB-231 cells that exhibit a typical mesenchymal phenotype (E-cadherin^{-} vimentin^{+}) in SCID mice and allowed metastases to develop in the lungs. Notably, MDA-derived metastases exhibited an E-cadherin^{+} epithelial phenotype (Figure S12A-B), suggesting that MDA-MB-231 cells have undergone MET in the lung environment. In this context, analysis of lung metastases from breast cancer patients also showed E-cadherin^{+} and vimentin^{-} metastases (Figure S12C). Based on these observations, we hypothesized that myeloid cells recruited in the premetastatic lungs produce versican which induces MET in tumor cells to promote tumor outgrowth.

To determine whether versican-mediated MET is necessary for metastases formation *in vivo*, we injected luciferase/RFP labeled MDA-MB-231 cells *via* tail vein in SCID mice and monitored metastases progression either in the presence of versican (control IgG treated mice) or in lack of versican-producing myeloid cells (anti-Gr1 treated mice). Depletion of Gr1^{+} myeloid cells significantly impaired progression of metastases by >5-fold. (Figure 5A-B). Of note, the anti-Gr1 antibody treatment significantly inhibited the upregulated versican expression in the metastatic lungs (Figure 5C). Further evaluation of the lungs showed that macroscopic E-cadherin^{+}/vimentin^{low} metastatic lesions were generated by MDA-MB-231 cells in the presence of versican (Figure 5D, top panel) as expected. However, versican deficiency resulted in microscopic vimentin^{high}/E-cadherin^{-} lesions (Figure 5D, bottom panel) indicating a failure of MET. To confirm that the MET-induced accelerated metastasis was mainly due to versican, we performed a versican gain of function experiment. We injected MDA-MB-231 cell expressing a secreted form of versican V1 isoform (MDA-Vcn) and MDA-Cont cells *via* tail vein in SCID mice. Bioluminescence imaging (BLI) analysis revealed accelerated progression (>4 fold) of lung metastases with MDA-Vcn cells compared to MDA-Cont cells (Figure 5E-F).

Taken together, these results suggest that versican promotes MET of metastatic tumor cells and enhances progression into macrometastatic lesions.

Myeloid cells express versican in the metastatic lungs of breast cancer patients.

Next, we asked whether metastatic lungs of breast cancer patients exhibit elevated levels of versican as observed in mouse models. Immunohistochemical analysis showed enhanced versican in the metastatic lungs of breast cancer patients but not in lungs of normal healthy controls (Figure 6A). IHC analysis of metastatic lungs showed that versican expression was confined to the vicinity of CD11b^{+} myeloid cell clusters (Figure 6B). Using a cohort of breast cancer patients who have developed lung (n=6) or liver (n=11) metastases, we quantified versican expression by RT-PCR. Significantly higher versican expression was detected in metastatic organs as compared to normal tissues (5.8±1.3 and 6.5±1.5 fold in the liver and lung metastasis respectively, Figure 6C). We further evaluated whether a subset of CD11b^{+} cells expressed versican in cancer patients. Given that Gr1 is not expressed in humans, myeloid cells are defined by the coexpression of CD11b and CD33 (20). Indeed, flow cytometry analysis showed that the CD11b^{+}CD33^{+} cells that comprise the monocytic

population expressed versican, while the $CD11b^{+}CD33^{-}$ fraction or the pure tumor cells did not (Figure 6D-E). These results suggest that as observed in mouse models, versican expressed by tumor elicited myeloid cells may contribute to metastasis in cancer patients.

Discussion

We have shown BM-derived $CD11b^{+}GR1^{+}$ myeloid progenitor cells recruited to the premetastatic lungs promote tumor outgrowth. Various protumorigenic activities have been associated with $Gr1^{+}$ myeloid cells, including expression of proangiogenic factor BV8 (32), metastasis-promoting Lysyl oxidase and MMP9 (33), contribution to TGFβ-mediated metastasis (34), and immune tolerance and suppression by virtue of innate MDSC activity (35, 36). Here, we have identified a novel role for the recruited $Gr1^{+}$ myeloid cells in mediating tumor outgrowth in metastatic lungs. By secreting versican, the $Ly6C^{high}$ monocytic subpopulation of Gr1+ myeloid cells, in a paracrine fashion, promoted cell proliferation and induced MET of tumor cells (Figure 7). Importantly, versican deficiency in the Gr1+ cells did not block their recruitment to the lung microenvironment; neither did it alter the immune microenvironment of the lung as determined by evaluation of key cell types and immune mediators suggesting that the MDSC activity of these cells was not compromised. However, versican knockdown in myeloid cells or specific depletion of versican producing myeloid cells significantly impaired macrometastases formation.

In the metastatic lungs the major contributors of versican were $CD11b^{+}Ly6C^{high}$ cells. While the fibroblasts expressed versican as observed in previous studies(23-25), the contribution of fibroblasts to the metastatic lung was about 10-fold lower compared to $CD11b^{+}Ly6C^{high}$ cells, and no significant increase in numbers was observed in the metastatic lungs compared to controls (Figure S4B). Consistent with these observations, versican knockdown specifically in the BM significantly impaired lung metastasis *in vivo*. However, in one report versican expression by LLC cells promoted metastasis (37). Our analysis of a panel of tumor cell lines from breast, prostate, colon, and lung cancer showed that versican expression in tumor cells is significantly lower compared with myeloid cells. Based on all these results we conclude that the $Ly6C^{high}$ myeloid cells are the major contributors of versican in metastatic lungs in both mouse and human (Figure 2, Figure 6 and Figure S4C). MET plays an important role in development (38), however the MET cascade has not been demonstrated in tumor metastasis. In this study, we have observed E-$cadherin^{+}$ and $vimentin^{-}$ metastatic lesions both in mice and human. Consistently, in a recent study IHC analysis of many human primary lung tumors, and their brain metastases showed increased epithelial to mesenchymal ratios in metastatic lesions compared with advanced primary tumors (39). Thus, our observation that versican stimulates MET of metastatic tumor cells explains, in part, the observations that cancer cells in distant metastases exhibit an epithelial phenotype resembling the primary tumor from which they arose. Our study has also addressed the speculation in the field that metastatic tumor cells recruited to distal target organs undergo a reverse EMT often referred to as MET (9, 30, 31). However, technological limitations such as lack of robust markers to track single disseminated tumor cells that have undergone EMT to the metastatic site in patients preclude a detailed analysis of MET in humans, further exacerbated with limitations in non-invasive dynamic imaging at the single cell level.

We have also explored the mechanism by which versican induces MET. Versican attenuated the Smad-mediated EMT signaling pathway as determined by the reduction of p-Smad2 levels and suppression of transcription factor Snail. The suppression of Smad2 pathway-induced MET, increased cell proliferation consistent with previous reports (40, 41). In addition, versican did not impact apoptosis (data not shown), suggesting that versican-mediated stimulation of MET and enhanced proliferation may be the main mechanism of increased tumor outgrowth and formation of focal macrometastases. Analysis of a cohort of breast cancer patients from whom distal metastases were available showed clusters of myeloid cells expressing versican in the metastatic lungs. Consistent with IHC, RT-PCR analysis showing enhanced versican expression in metastatic lungs, brain, and liver in breast cancer patients compared to control normal lungs. These observations suggest that versican expression in the metastatic organ may be used to predict survival, given the relationship between metastases and poor survival in breast cancer patients. However, such an analysis is challenging at the present time due to limited availability of human metastatic lesions, and future studies are required to expand the analysis in a much larger cohort of breast cancer patients to determine with statistical confidence whether increased levels of versican expression in the lungs correlate with poor survival.

Given that the initial colonization by disseminated tumor cells has occurred in many patients at the time of primary tumor diagnosis, our results suggest that selectively targeting tumor-elicited myeloid cells or versican-mediated proliferation pathways, perhaps in combination with conventional chemotherapeutics, may represent a potential therapeutic strategy for combating metastatic disease.

Supplementary Material

Refer to Web version on PubMed Central for supplementary material.

Acknowledgments

We thank Dr. Zimmermann (University of Zurich) for human versican cDNA clone and Dr. Anna Durrans for valuable comments on the manuscript.

Grant Support

Work was partly supported by Neuberger Berman Lung Cancer Laboratory, the Robert I. Goldman Foundation and Cornell Center on the Microenvironment and Metastasis through Award Number U54CA143876 from the NCI (V.Mittal).

References:

1. Townson JL, Chambers AF. Dormancy of solitary metastatic cells. Cell Cycle. 2006;5:1744–50. [PubMed: 16861927]
2. Naumov GN, Bender E, Zurakowski D, Kang SY, Sampson D, Flynn E, et al. A model of human tumor dormancy: an angiogenic switch from the nonangiogenic phenotype. J Natl Cancer Inst. 2006;98:316–25. [PubMed: 16507828]
3. Gupta GP, Massague J. Cancer metastasis: building a framework. Cell. 2006;127:679–95. [PubMed: 17110329]
4. Joyce JA, Pollard JW. Microenvironmental regulation of metastasis. Nat Rev Cancer. 2009;9:239–52. [PubMed: 19279573]

5. Polyak K, Weinberg RA. Transitions between epithelial and mesenchymal states: acquisition of malignant and stem cell traits. Nat Rev Cancer. 2009;9:265–73. [PubMed: 19262571]
6. Fidler IJ. The pathogenesis of cancer metastasis: the 'seed and soil' hypothesis revisited. Nat Rev Cancer. 2003;3:453–8. [PubMed: 12778135]
7. Kaplan RN, Psaila B, Lyden D. Bone marrow cells in the 'pre-metastatic niche': within bone and beyond. Cancer Metastasis Rev. 2006;25:521–9. [PubMed: 17186383]
8. Gao D, Nolan DJ, Mellick AS, Bambino K, McDonnell K, Mittal V. Endothelial progenitor cells control the angiogenic switch in mouse lung metastasis. Science. 2008;319:195–8. [PubMed: 18187653]
9. Chaffer CL, Thompson EW, Williams ED. Mesenchymal to epithelial transition in development and disease. Cells Tissues Organs. 2007;185:7–19. [PubMed: 17587803]
10. Dutt S, Cassoly E, Dours-Zimmermann MT, Matasci M, Stoeckli ET, Zimmermann DR. Versican V0 and V1 direct the growth of peripheral axons in the developing chick hindlimb. J Neurosci. 2011;31:5262–70. [PubMed: 21471361]
11. Guy CT, Cardiff RD, Muller WJ. Induction of mammary tumors by expression of polyomavirus middle T oncogene: a transgenic mouse model for metastatic disease. Mol Cell Biol. 1992;12:954–61. [PubMed: 1312220]
12. Nolan DJ, Ciarrocchi A, Mellick AS, Jaggi JS, Bambino K, Gupta S, et al. Bone marrow-derived endothelial progenitor cells are a major determinant of nascent tumor neovascularization. Genes Dev. 2007;21:1546–58. [PubMed: 17575055]
13. Wight TN. Versican: a versatile extracellular matrix proteoglycan in cell biology. Curr Opin Cell Biol. 2002;14:617–23. [PubMed: 12231358]
14. Ricciardelli C, Brooks JH, Suwiwat S, Sakko AJ, Mayne K, Raymond WA, et al. Regulation of stromal versican expression by breast cancer cells and importance to relapse-free survival in patients with node-negative primary breast cancer. Clin Cancer Res. 2002;8:1054–60. [PubMed: 11948113]
15. Suwiwat S, Ricciardelli C, Tammi R, Tammi M, Auvinen P, Kosma VM, et al. Expression of extracellular matrix components versican, chondroitin sulfate, tenascin, and hyaluronan, and their association with disease outcome in node-negative breast cancer. Clin Cancer Res. 2004;10:2491–8. [PubMed: 15073129]
16. Pukkila M, Kosunen A, Ropponen K, Virtaniemi J, Kellokoski J, Kumpulainen E, et al. High stromal versican expression predicts unfavourable outcome in oral squamous cell carcinoma. J Clin Pathol. 2007;60:267–72. [PubMed: 16731595]
17. Kodama J, Hasengaowa, Kusumoto T, Seki N, Matsuo T, Ojima Y, et al. Prognostic significance of stromal versican expression in human endometrial cancer. Ann Oncol. 2007;18:269–74. [PubMed: 17065588]
18. Pirinen R, Leinonen T, Bohm J, Johansson R, Ropponen K, Kumpulainen E, et al. Versican in nonsmall cell lung cancer: relation to hyaluronan, clinicopathologic factors, and prognosis. Hum Pathol. 2005;36:44–50. [PubMed: 15712181]
19. Pukkila MJ, Kosunen AS, Virtaniemi JA, Kumpulainen EJ, Johansson RT, Kellokoski JK, et al. Versican expression in pharyngeal squamous cell carcinoma: an immunohistochemical study. J Clin Pathol. 2004;57:735–9. [PubMed: 15220367]
20. Krystal G, Sly L, Antignano F, Ho V, Ruschmann J, Hamilton M. Re: the terminology issue for myeloid-derived suppressor cells. Cancer Res. 2007;67:3986. [PubMed: 17440115]
21. Gabrilovich DI, Bronte V, Chen SH, Colombo MP, Ochoa A, Ostrand-Rosenberg S, et al. The terminology issue for myeloid-derived suppressor cells. Cancer Res. 2007;67:425; author reply 6. [PubMed: 17210725]
22. Coffelt SB, Lewis CE, Naldini L, Brown JM, Ferrara N, De Palma M. Elusive identities and overlapping phenotypes of proangiogenic myeloid cells in tumors. Am J Pathol. 2010;176:1564–76. [PubMed: 20167863]
23. Ricciardelli C, Sakko AJ, Ween MP, Russell DL, Horsfall DJ. The biological role and regulation of versican levels in cancer. Cancer Metastasis Rev. 2009;28:233–45. [PubMed: 19160015]
24. Zimmermann DR, Ruoslahti E. Multiple domains of the large fibroblast proteoglycan, versican. EMBO J. 1989;8:2975–81. [PubMed: 2583089]

25. Sheng W, Wang G, Wang Y, Liang J, Wen J, Zheng PS, et al. The roles of versican V1 and V2 isoforms in cell proliferation and apoptosis. Mol Biol Cell. 2005;16:1330–40. [PubMed: 15635104]
26. Padua D, Massague J. Roles of TGFbeta in metastasis. Cell Res. 2009;19:89–102. [PubMed: 19050696]
27. Shi Y, Massague J. Mechanisms of TGF-beta signaling from cell membrane to the nucleus. Cell. 2003;113:685–700. [PubMed: 12809600]
28. Song J EMT or apoptosis: a decision for TGF-beta. Cell Res. 2007;17:289–90. [PubMed: 17426696]
29. Hata A, Shi Y, Massague J. TGF-beta signaling and cancer: structural and functional consequences of mutations in Smads. Mol Med Today. 1998;4:257–62. [PubMed: 9679244]
30. Hugo H, Ackland ML, Blick T, Lawrence MG, Clements JA, Williams ED, et al. Epithelial--mesenchymal and mesenchymal--epithelial transitions in carcinoma progression. J Cell Physiol. 2007;213:374–83. [PubMed: 17680632]
31. Chaffer CL, Brennan JP, Slavin JL, Blick T, Thompson EW, Williams ED. Mesenchymal-to-epithelial transition facilitates bladder cancer metastasis: role of fibroblast growth factor receptor-2. Cancer Res. 2006;66:11271–8. [PubMed: 17145872]
32. Kowanetz M, Wu X, Lee J, Tan M, Hagenbeek T, Qu X, et al. Granulocyte-colony stimulating factor promotes lung metastasis through mobilization of Ly6G+Ly6C+ granulocytes. Proc Natl Acad Sci U S A. 2010;107:21248–55. [PubMed: 21081700]
33. Erler JT, Bennewith KL, Cox TR, Lang G, Bird D, Koong A, et al. Hypoxia-induced lysyl oxidase is a critical mediator of bone marrow cell recruitment to form the premetastatic niche. Cancer Cell. 2009;15:35–44. [PubMed: 19111879]
34. Yang L, Huang J, Ren X, Gorska AE, Chytil A, Aakre M, et al. Abrogation of TGF beta signaling in mammary carcinomas recruits Gr-1+CD11b+ myeloid cells that promote metastasis. Cancer Cell. 2008;13:23–35. [PubMed: 18167337]
35. Ostrand-Rosenberg S, Sinha P. Myeloid-derived suppressor cells: linking inflammation and cancer. J Immunol. 2009;182:4499–506. [PubMed: 19342621]
36. Youn JI, Nagaraj S, Collazo M, Gabrilovich DI. Subsets of myeloid-derived suppressor cells in tumor-bearing mice. J Immunol. 2008;181:5791–802. [PubMed: 18832739]
37. Kim S, Takahashi H, Lin WW, Descargues P, Grivennikov S, Kim Y, et al. Carcinoma-produced factors activate myeloid cells through TLR2 to stimulate metastasis. Nature. 2009;457:102–6. [PubMed: 19122641]
38. Vainio S, Lin Y. Coordinating early kidney development: lessons from gene targeting. Nat Rev Genet. 2002;3:533–43. [PubMed: 12094231]
39. Prudkin L, Liu DD, Ozburn NC, Sun M, Behrens C, Tang X, et al. Epithelial-to-mesenchymal transition in the development and progression of adenocarcinoma and squamous cell carcinoma of the lung. Mod Pathol. 2009;22:668–78. [PubMed: 19270647]
40. Mur C, Martínez-Carpio PA, Fernández-Montolí ME, Ramon JM, Rosel P, Navarro MA. Growth of MDA-MB-231 cell line: different effects of TGF-beta(1), EGF and estradiol depending on the length of exposure. Cell Biol Int. 1998;22:679–84. [PubMed: 10452838]
41. Zugmaier G, Ennis BW, Deschauer B, Katz D, Knabbe C, Wilding G, et al. Transforming growth factors type beta 1 and beta 2 are equipotent growth inhibitors of human breast cancer cell lines. J Cell Physiol. 1989;141:353–61. [PubMed: 2808542]

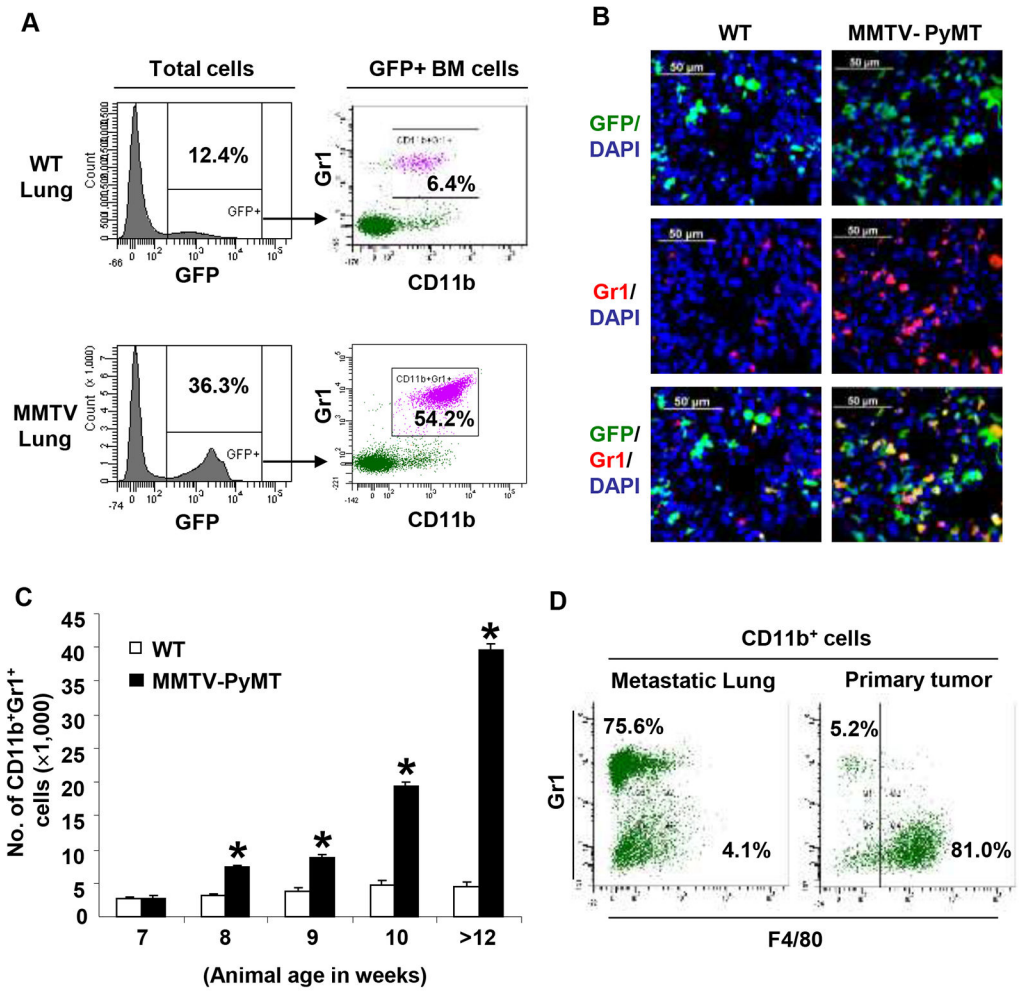

Figure 1. Myeloid cells are recruited to the lung in MMTV-PyMT mice.

A, Flow cytometry plots showing increased recruitment of BM-derived (GFP^+) $CD11b^+Gr1^+$ myeloid cells in the lungs of MMTV-PyMT mice (12 weeks old) compared to wild type (WT) mice. Representative plots were derived from three independent experiments.

B, Immunostaining showing increased recruitment of BM-derived GFP^+Gr1^+ cells in the lungs of MMTV-PyMT mice compared to WT mice.

C, Kinetic analysis of the recruitment of $CD11b^+Gr1^+$ myeloid cells in the lungs of MMTV-PyMT mice (age in weeks). The numbers of $CD11b^+Gr1^+$ cells were normalized to 1×10^5 total lung cells analyzed per animal. Mean±s.d. *$p<0.01$ as compared to WT mice of same age.

D, Flow cytometry analysis showing the majority of myeloid cells are $Gr1^+F4/80^-$ in the metastatic lung, but are $Gr1^-F4/80^+$ macrophages in the primary tumors.

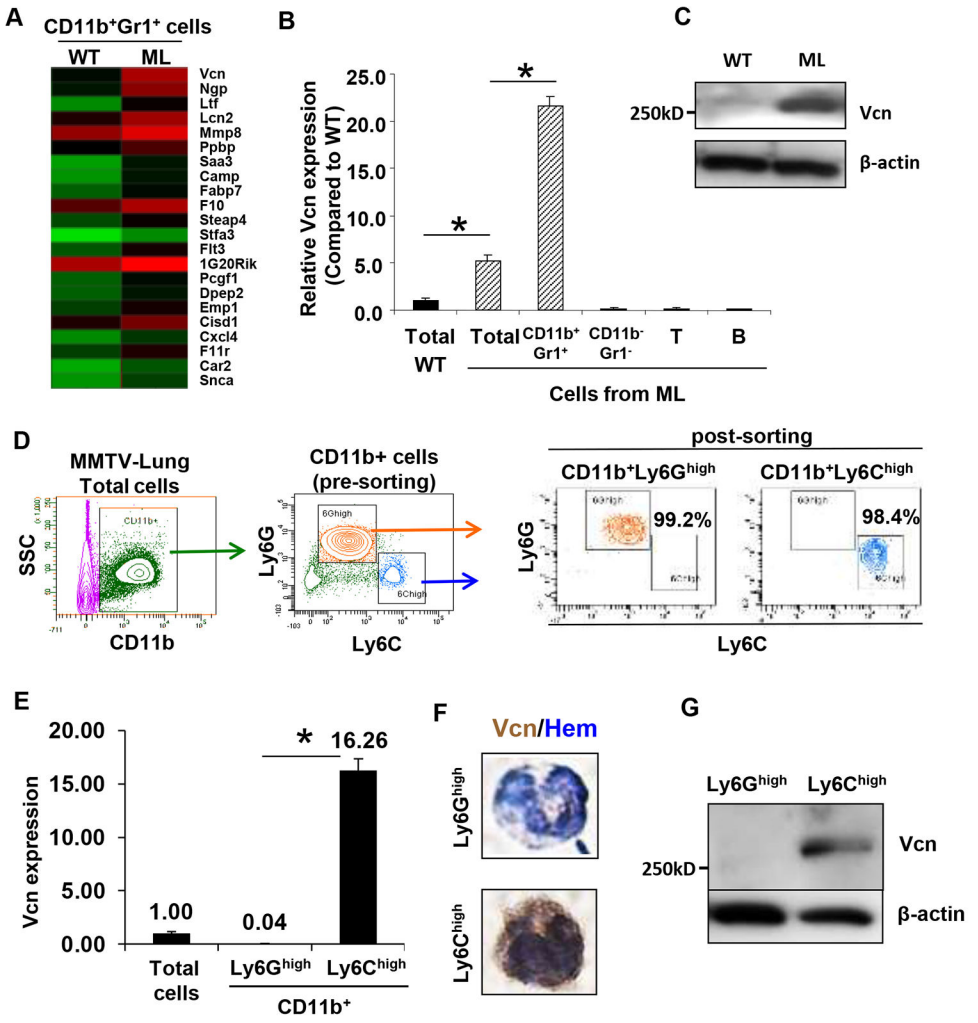

Figure 2. Versican is expressed by CD11b^{+}Ly6C^{high} myeloid cells in the metastatic lung.

A, Heat map obtained from gene expression profiling of CD11b^{+}Gr1^{+} cells sorted from WT lungs and metastatic lungs (ML). Each row represents a differentially upregulated gene (≥ 2 fold) in ML samples, and each column represents data from one comparison (average of three biological replicates). Red, high expression; Green, low expression.

B, RT-PCR showing versican expression in Gr1^{+} myeloid cells, Gr1^{-} stromal cells, T cells (CD3^{+}) and B cells (B220^{+}) sorted from WT or ML (representative data from two individual experiments). Versican expression was normalized to the internal control (GAPDH). The relative expression level is shown as compared to WT lung, *p<0.01 as indicated.

C, Western blot showing versican levels in the lungs from MMTV-PyMT mice and control mice.

D, Left panels, Flow cytometry sorting of CD11b^{+}Ly6G^{high} and CD11b^{+}Ly6C^{high} cells from the lungs of MMTV-PyMT mice. Right panels, Flow cytometry showing purity of the post-sorted cells.

E, RT-PCR of versican expression in CD11b^{+}Ly6G^{high} and CD11b^{+}Ly6C^{high} cells and total cells from metastatic lungs. GAPDH was used as internal control. Representative data is from three independent experiments. *p<0.01.

F, IHC of versican on $CD11b^{+}Ly6G^{high}$ and $CD11b^{+}Ly6C^{high}$ cells. Hematoxylin (Hem) was used to determine the morphology of the nucleus.
G, Western blot showing versican in sorted $CD11b^{+}Ly6G^{high}$ and $CD11b^{+}Ly6C^{high}$ cells from metastatic lungs of MMTV-PyMT mice.

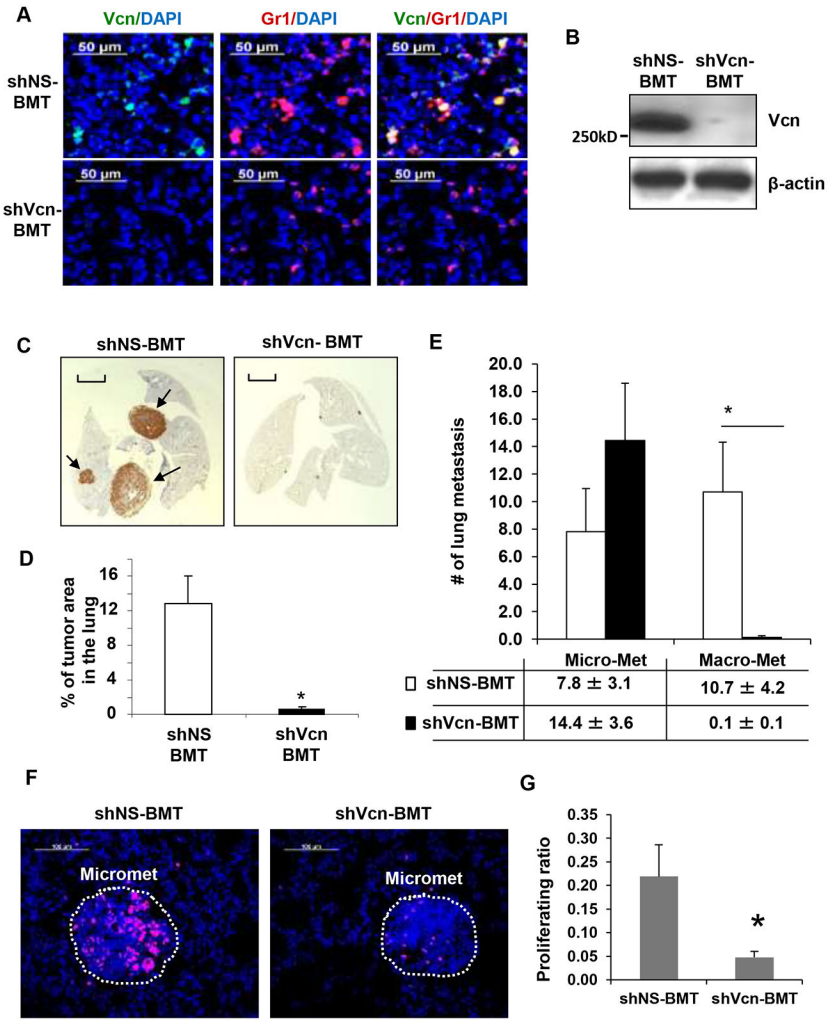

Figure 3. Versican deficiency in myeloid cells impairs macrometastases in MMTV-PyMT mice.

A, Representative microscopy images showing versican (green) deficiency in $Gr1^{+}$(red) cells in the lungs of shVcn-BMT MMTV-PyMT mice compared to shNS-BMT mice (10-weeks old).

B, Western blots showing versican in the lungs from shNS-BMT and shVcn-BMT MMTV-PyMT mice.

C, Representative lung images (stained with anti-PyMT antibody) of shNS-BMT and shVcn-BMT MMTV-PyMT mice (15-weeks old). Arrows mark pulmonary metastases. Scale bar, 2mm.

D, Quantitation of the area of metastases in shNS-BMT and shVcn-BMT MMTV-PyMT mice (15-weeks old, n=7-9 per group, *p<0.01 as compared to shNS-BMT group).

E, Quantitation of the number of metastases in shNS-BMT and shVcn-BMT MMTV-PyMT mice. The average number of micrometastasis (<1mm in diameter) and macrometastasis (>1mm in diameter) were counted from at least 5 sections from individual animals, n = 7-9, *p<0.01 as compared to shNS-BMT group.

F, Staining of Ki67 (magenta) showing proliferating cells in the micrometastases in lungs of shNS-BMT mice as compared with that from shVcn-BMT mice.

G, Quantification of the proliferation ratio in micrometastases showing less proliferating cells in lesions from shVcn-BMT mice compared to shNS-BMT mice. n=10, *p<0.01.

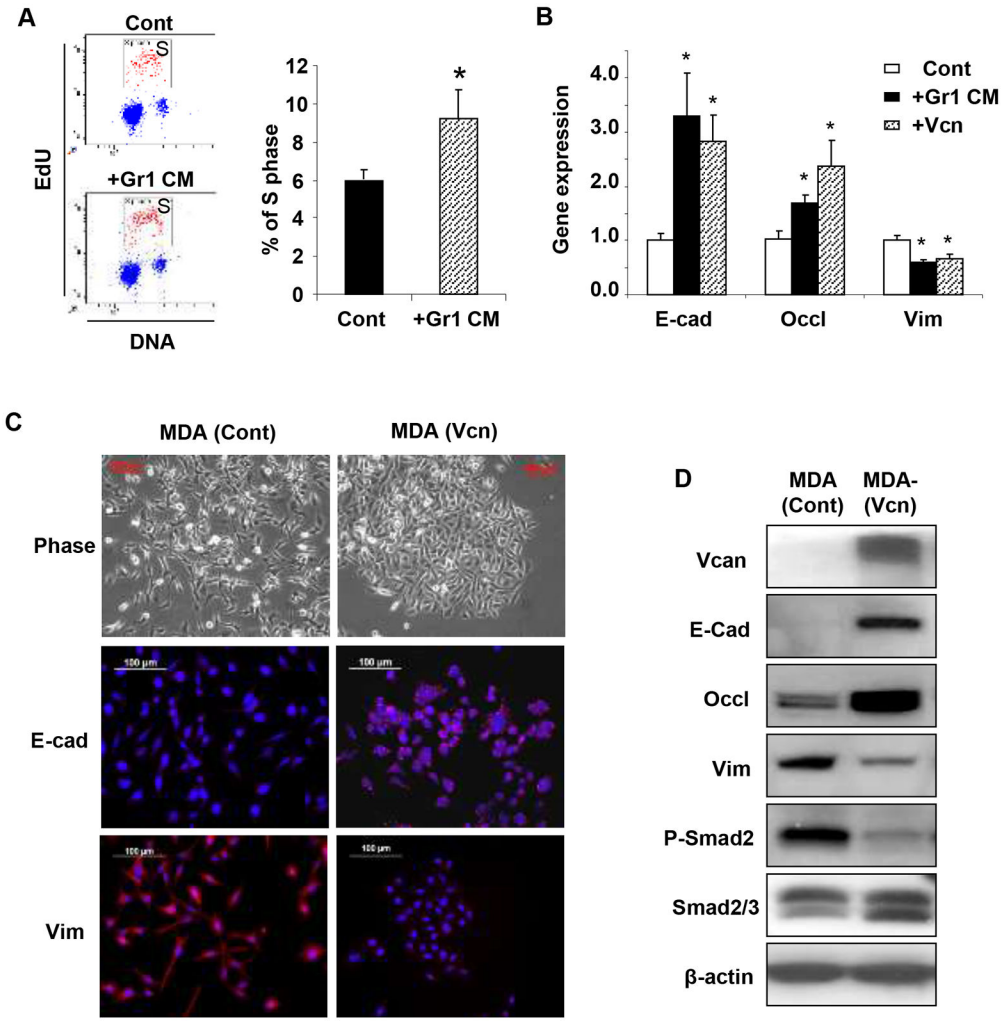

Figure 4. Versican enhances proliferation and induces MET in metastatic tumor cells.

A, Flow cytometry plots depicting cell cycle analysis of metastatic breast cancer MDA-MB-231 cells treated with Gr1+ CM or control media (Cont). Percentage of S phase cells are indicated. Representative plots are from 3 experiments.

B, Quantitative RT-PCR analysis of epithelial/mesenchymal marker expression in MDA-MB-231 cells treated with Gr1 CM, or biochemically purified versican (+Vcn, 2.5 μg/mL). n=3, *p<0.01 as compared to untreated cells (Cont).

C, Microscopy images of MDA-control cells and MDA-versican cells (MDA-Vcn) depicting morphology (Phase) and expression of epithelial/mesenchymal markers. E-cad,E-cadherin; Vim,vimentin.

D, Western blot analysis of versican (>250 KDa), EMT markers, phospho (p)-Smad2, and total Smad2/3 expression in MDA (Vcn) cells and MDA (Cont) cells. Representative data from three experiments.

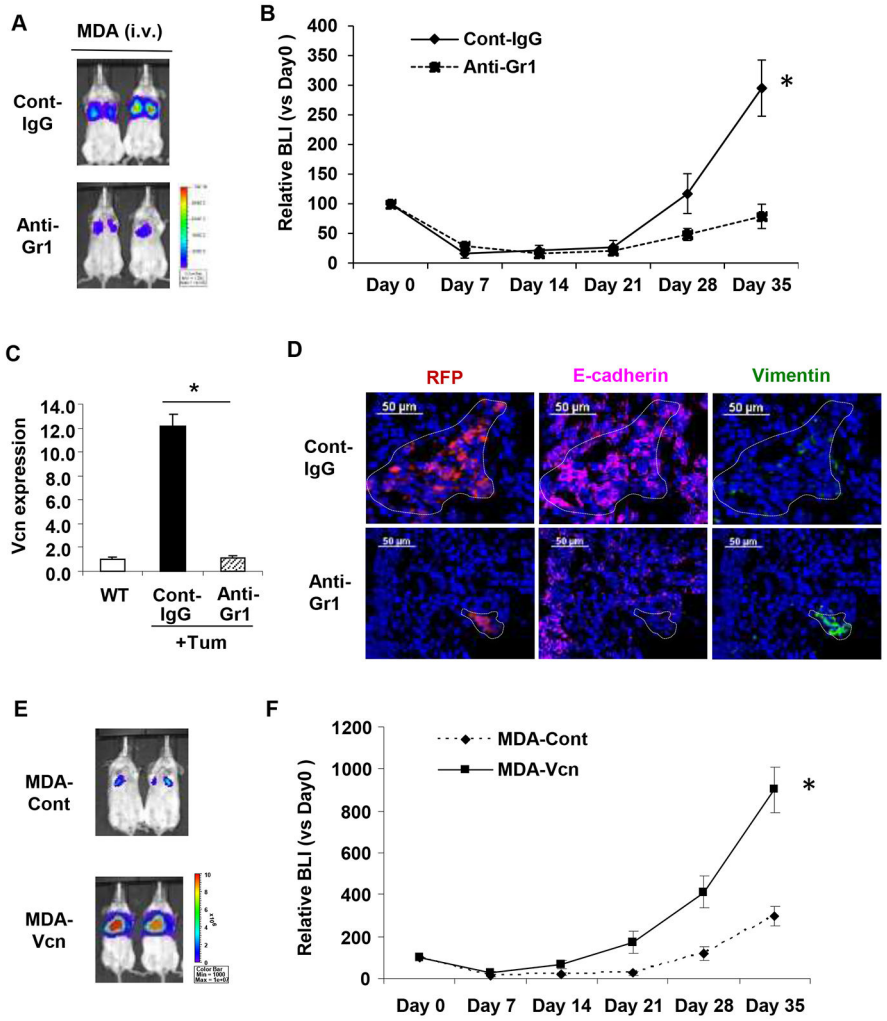

Figure 5. Versican deficiency impairs MET-mediated lung metastases *in vivo*.

A, BLI images showing that depletion of versican-producing Gr1+ cells by anti-Gr1 antibody treatment inhibited lung metastases formed by MDA-MB-231 cells compared to IgG treated controls. Scale bar depicts the photon flux (photons per second).

B, Quantification of pulmonary metastases by BLI at days 0,7,14,21,28,35 after inoculation. The relative BLIs are normalized using the values from day 0, n=10. *p<0.01.

C, Myeloid cells harvested from WT and control antibody treated (Cont-IgG) or anti-Gr1 antibody treated (Anti-Gr1) tumor-bearing animals. Versican expression was analyzed by RT-PCR (n=3 in each group). GAPDH was used as internal control for RT-PCR. *p<0.01 as indicated.

D, Images showing expression of E-cadherin (magenta) and vimentin (green) in pulmonary metastases formed by MDA-MB-231 cells in mice treated with control IgG or anti-Gr1 antibodies. Tumor cells were detected by the intrinsic RFP signal (red). The metastatic lesions are shown within the dotted line. Note that lung epithelial cells surrounding the metastases also stain for E-cadherin.

E, Versican promotes lung metastasis in vivo. Representative bioluminiscence images showing accelerated metastases of MDA-Vcn cells in the lung after tail vein injection as compared to MDA-Cont cells (n=5).

F, Quantification of pulmonary metastases by BLI at days 0,7,14,21,28,35 after inoculation. The relative BLIs are normalized using the values from day 0, n=5, *P<0.01.

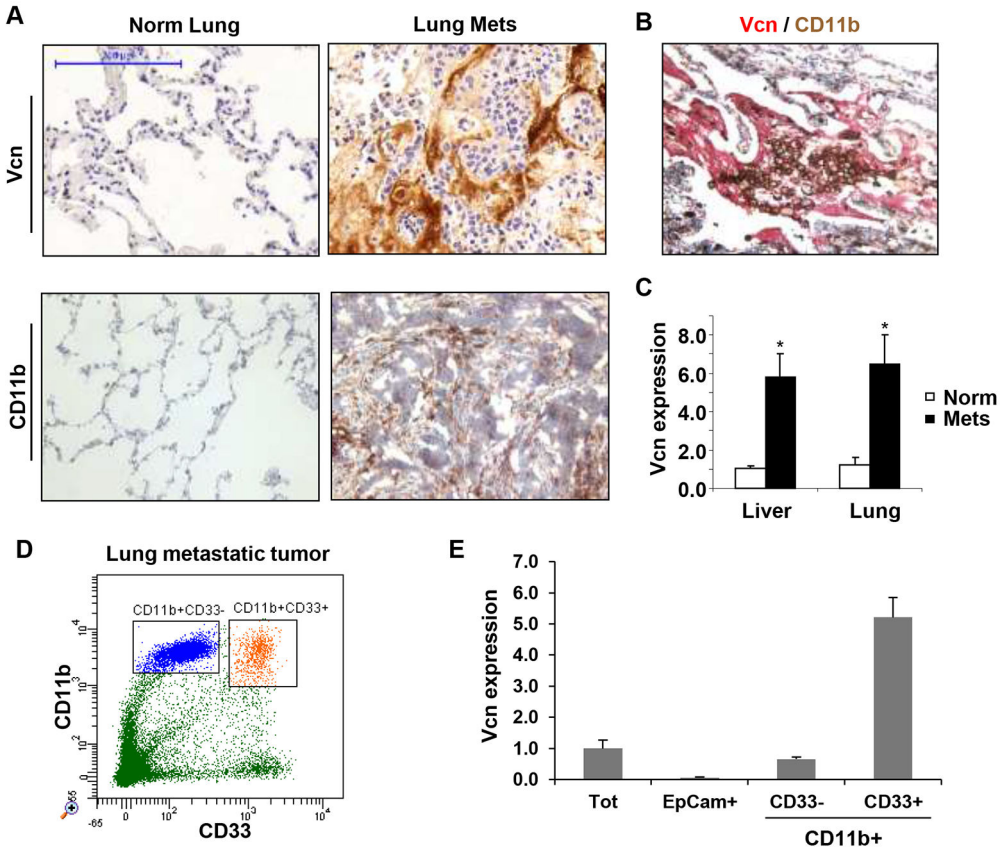

Figure 6. Versican expression in the metastatic tumors of breast cancer patients.

A, Representative IHC images of lungs from normal healthy subjects (Normal Lung, n=5) and breast cancer patients with metastases (Lung Mets, n=11) showing stromal versican expression. Scale bar,200μm.

B, IHC of lung metastases from a breast cancer patient showing colocalization of recruited $CD11b^+$ (brown) myeloid cells with versican (red).

C, Quantification of versican expression by RT-PCR in lung metastases (n=6) and liver metastases (n=11) of breast cancer patients as compared to healthy normal tissues (n=5, n=4 respectively).

D, Flow cytometry showing that $CD11b^+$ cells in the human metastatic lungs are comprised of $CD11b^+CD33^+$ and $CD11b^+CD33^-$ populations.

E, RT-PCR of versican expression in sorted total cells (Tot), tumor cells ($EpCam^+$), $CD11b^+CD33^+$ myeloid cells, and $CD11b^+CD33^-$ cells in a breast cancer patient with lung metastases.

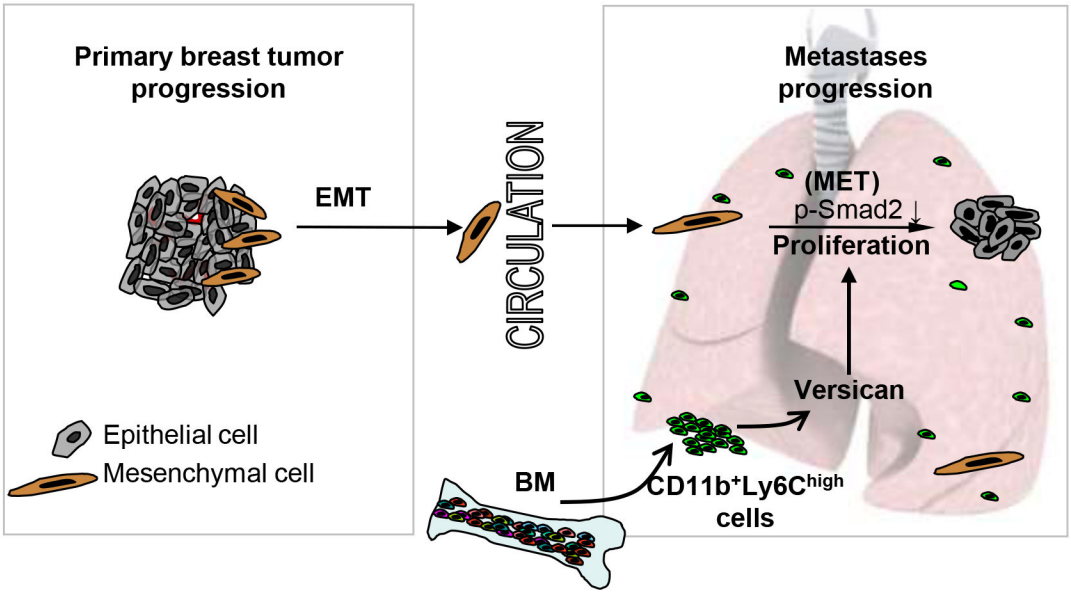

Figure 7. Schematic depicting the contribution of BM-derived myeloid cells to the formation of lung metastases from breast tumor.

EMT,epithelial to mesenchymal transition; MET,mesenchymal to epithelial transition; BM,bone marrow; p-Smad2, phospho-Smad2.